Aerosol and Air Quality Research, 19: 2222–2238, 2019

ISSN: 1680-8584 print / 2071-1409 online
doi: 10.4209/aaqr.2019.02.0076

Chemical Characteristics, Sources Apportionment, and Risk Assessment of $PM_{2.5}$ in Different Functional Areas of an Emerging Megacity in China

Xiaohan Liu, Nan Jiang*, Xue Yu, Ruiqin Zhang, Shengli Li, Qiang Li, Panru Kang

Key Laboratory of Environmental Chemistry and Low Carbon Technologies of Henan Province, Research Institute of Environmental Science, College of Chemistry and Molecular Engineering, Zhengzhou University, Zhengzhou 450001, China

ABSTRACT

The mass concentration, chemical composition, and source apportionment of $PM_{2.5}$ in the urban, industrial, scenic, traffic, and rural sites of Zhengzhou were studied from February to December of 2016. The average annual concentration of $PM_{2.5}$ in these five sites was 119 μg m^{-3}, which was lower than the annual average between 2013 and 2015. However, $PM_{2.5}$ pollution remains serious in Zhengzhou. $PM_{2.5}$, elemental carbon (EC), organic carbon (OC), and water-soluble inorganic ions (WSIIs)—with the exception of F^-, Ca^{2+}, and Mg^{2+}—showed a relatively homogeneous spatial distribution in this area. Among these pollutants, WSIIs, carbonaceous species (EC and OC), and elements accounted for 47.7%, 14.4%, and 9.6% of $PM_{2.5}$ concentration in Zhengzhou, respectively. The annual OC/EC ratio in Zhengzhou was 8.3, which indicates the possible presence of a secondary organic carbon. Six main sources of $PM_{2.5}$ in Zhengzhou, namely, soil dust (15.1%), coal combustion (17.6%), secondary aerosol (35.1%), vehicle traffic (17.3%), industry (7.3%), and biomass burning (7.7%), were identified by using a positive matrix factorization model. The results of the back trajectory and potential source contribution function analysis revealed that the air mass from regions of the Shandong and Hubei Provinces aggravated the pollution in Zhengzhou, and Puyang, Hebi, Xinxiang, and Kaifeng were the main potential sources of $PM_{2.5}$, respectively. The carcinogenic risks of As to children through the ingestion pathway exceeded the acceptable level. The findings of this work can provide an in-depth understanding of the $PM_{2.5}$ pollution in Zhengzhou.

Keywords: $PM_{2.5}$; Spatial distribution; Positive matrix factorization; Coefficients of divergence; Health risk assessment.

INTRODUCTION

China's economy has grown rapidly over the past decade and has propelled a rapid increase in the amount of air pollutant emissions from anthropogenic sources (Zhou *et al.*, 2016). Atmospheric particulate matter (PM), especially $PM_{2.5}$, is a primary air pollutant that has received significant attention because of its negative effects on human health, visibility, and climate change (Pope and Dockery, 2006; Bytnerowicz *et al.*, 2007; Mohsenibandpi *et al.*, 2017; Jiang *et al.*, 2019b; Li *et al.*, 2019). The diverse effects of $PM_{2.5}$ may be ascribed to its complex chemical components, such as its water-soluble inorganic ions (WSIIs), elements, carbonaceous substances, and organic components (Wang *et al.*, 2009; Zhang *et al.*, 2016; Liu *et al.*, 2017; Jiang *et al.*, 2018b). Fully understanding the chemical composition of $PM_{2.5}$ can help identify the sources (Jiang *et al.*, 2018e) and effectively control this pollutant (Yang *et al.*, 2011). Introduced by Paatero and Tapper, positive matrix factorization (PMF) is a sources allocation receptor model that is widely used for identifying the main sources of atmospheric pollutants in many places worldwide (Brown *et al.*, 2015; Contini *et al.*, 2016; Lan *et al.*, 2016; Jiang *et al.*, 2018d). Meanwhile, hybrid single-particle Lagrangian integrated trajectory (HYSPLIT) and potential source contribution function (PSCF) are important models for assessing the potential sources or regions of pollutants (Liu *et al.*, 2018; Jiang *et al.*, 2019a). Many studies have also examined the chemical characteristics and source distribution of $PM_{2.5}$ in the developed regions of China, including the Yangtze River Delta, Pearl River Delta, and Beijing-Tianjin-Hebei (Gu *et al.*, 2011; Zhang *et al.*, 2013; Li *et al.*, 2016; Tan *et al.*, 2016; Du *et al.*, 2017; Huang *et al.*, 2017). However, only few studies have examined the Central Plains Economic Region, where the atmospheric $PM_{2.5}$ have reached extremely serious levels (the annual average concentrations: 125–146 μg m^{-3}, Jiang *et al.*, 2017), especially in Zhengzhou (Ministry of Environmental Protection of the People's Republic of China, 2017). As the core city of the Central Plains Economic Region, Zhengzhou is located south of the North China Plain and in the lower reaches of the Yellow River

* Corresponding author.
E-mail address: jiangn@zzu.edu.cn

with a population of about 10 million. Zhengzhou has a rapidly growing economy with its Gross Domestic Product (GDP) increased from RMB 498.0 billion in 2011 to RMB 811.4 billion in 2016 (ZMBS, 2017). The leading industries in this city include equipment manufacturing, automobile, electronic information, biology and medicine, new materials, modern food manufacturing, aluminum and aluminum deep processing, home manufacturing, and brand clothing. From 2011 to 2016, the number of motor vehicles in Zhengzhou increased from 1.6 million to 2.7 million (ZMBS, 2017), which subsequently increased the emission of atmospheric pollutants in the city and resulted in a severe air pollution.

To date, only few studies have produced chemical speciation data for the $PM_{2.5}$ pollutants in Zhengzhou (Geng *et al.*, 2013; Jiang *et al.*, 2018c). Moreover, very few systematic studies have conducted multi-point analysis, source analysis, and health risk assessment of $PM_{2.5}$ components. Previous studies have highlighted many differences among the various sampling sites in the different functional areas of a single city. For instance, Han *et al.* (2015) found that the contribution of crustal elements in residential areas was higher than that in other regions, while the level of toxic metals in cement industrial areas was generally higher compared with that in other areas. A higher degree of $PM_{2.5}$ pollution is often in urban areas than in rural areas (Gao *et al.*, 2016). Given its significant role in promoting air pollution, conducting a chemical characterization and source apportionment of $PM_{2.5}$ in the different regions of Zhengzhou is imperative. Therefore, by exploring the chemical characteristics and source apportionment of $PM_{2.5}$ in different areas of Zhengzhou, this study produces very meaningful findings and conclusions for both researchers and policymakers.

The concentration, spatial distribution, and source apportionment of $PM_{2.5}$ in the rural, urban, industrial, scenic, and traffic areas of Zhengzhou are examined in this work. The five primary objectives of this work are to (1) understand the characteristics and spatial distributions of $PM_{2.5}$ and chemical species, (2) perform source apportionment by using the PMF model, (3) ascertain the potential source regions by using the PSCF model, (4) evaluate the health risk posed by toxic elements, and (5) analyze the various characteristics of heavy pollution days.

EXPERIMENTAL METHODS

Sampling Sites

$PM_{2.5}$ was collected in the rural, urban, industrial, scenic, and traffic sites of Zhengzhou from February to December of 2016 (Fig. 1). The scenic site, Dengfeng (DF), has relatively few industries located nearby and lies in the southwest suburb of Zhengzhou. As a traffic site, Hangkonggang (HKG) lies in the south suburb of the city and is located 3.6 km away from Xinzheng International Airport. Situated in the east suburb of Zhongshan, Zhongmu (ZM) is a rural site located near a large farmland area and has no obvious industrial source. Xinmi (XM), which lies in the southwest suburb of the city, acts as the important industrial site of Zhengzhou. The 47th middle school (SSQ) lies in the urban area of the city and is located near the convention center and main road. Table 1 presents detailed information about these sampling sites.

Sampling

Middle-volume sampling instruments (100 L min^{-1}; TH-150AII, Tianhong, China) were used to collect $PM_{2.5}$ samples from each site. Two sampling filter membranes were used, including polypropylene filters for analyzing the elements (90 mm in diameter; Tianjin Xinyao, China) and quartz microfiber filters for analyzing the other chemical constituents (90 mm in diameter; PALLLFLEX, USA). $PM_{2.5}$ samples were collected from 10 a.m. on the first day to 9 a.m. on the second day. Quartz filter before sampling in a muffle furnace at 450°C baking 5 h eliminate organic matter may affect.

The filter was placed in ultraclean room balance (20 ± 5°C temperature and 50 ± 5% relative humidity) for 48 h. Afterward, high-precision electronic weighing scales (Mettler Toledo XS205) with a weight difference of no more than 0.03 mg were used to weigh the samples twice to guarantee weighing precision. The samples were then stored in a freezer at –20°C before the analysis.

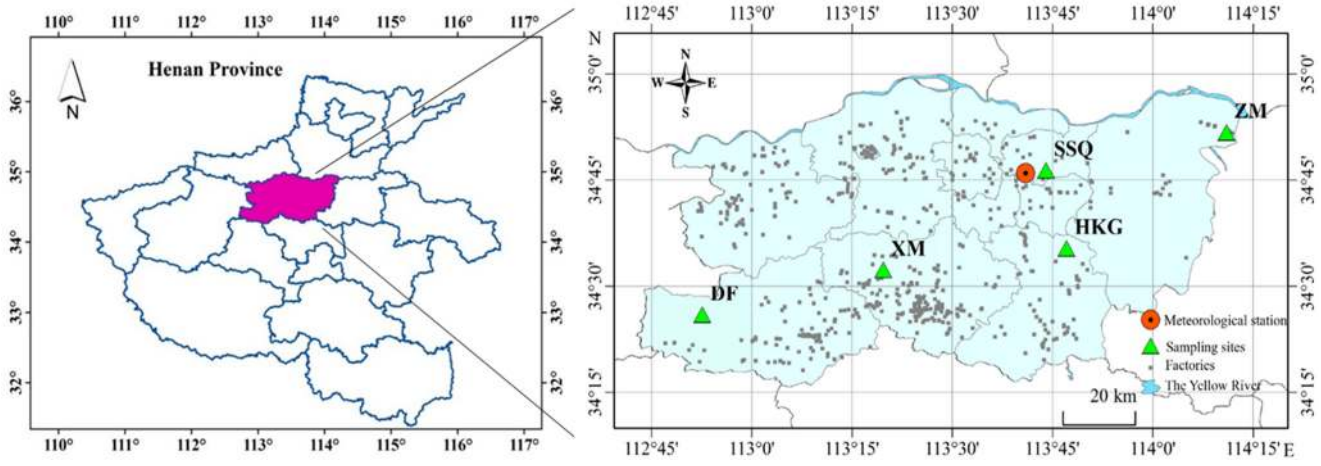

Fig. 1. Location of five sample sites.

Table 1. Description of $PM_{2.5}$ in the sampling sites in Zhengzhou.

Site	Site code	Coordinates	Site description	
Forty-seventh middle school	SSQ	Lat: N 34.46 Lon: E 113.44	Urban	Urban site, near Zhengzhou International Convention and Exhibition center, high traffic
Hangkonggang	HKG	Lat: N 34.34 Lon: E 113.51	Traffic	Traffic site, close to Xinzheng International Airport, greatly affected by aircraft fuel
Xinmi	XM	Lat: N 34.32 Lon: E 113.19	Industrial	adjacent to the main road (Xidajie) in Xinmi, the area is rich in industry
Dengfeng	DF	Lat: N 34.25 Lon: E 112.52	Scenic	Scenic site, located in the scenic area, about 400 meters from zheng-shao-luo highway
Zhongmu	ZM	Lat: N 34.51 Lon: E 114.16	Rural	Agricultural site, far from the city, there is no obvious industrial source nearby

Chemical Analysis

Half of each quartz filter sample was used to determine the concentrations of the nine WSIIs (F^-, Cl^-, NO_3^-, SO_4^{2-}, Na^+, NH_4^+, K^+, Mg^{2+}, and Ca^{2+}) via ion chromatography (ICS-90, ICS-900, Dionex, USA). More details can be found in Yu *et al.* (2018).

A 2.0 cm^2 filter was intersected with a punch in a quartz fiber filter, and then OC and EC were analyzed with a carbon analyzer (Sunset Laboratory, USA). Two temperature rise steps were performed in the analysis. This process is described in detail in Jiang *et al.* (2018a).

A total of 21 metallic compounds and elements (Na, Ba, Mg, Sb, Al, Sr, Si, K, Se, Ca, Ti, Ga, V, Ni, Pb, Cu, Zn, As, Fe, Mn, and Cr) in the filters were measured by using an S8 TIGER wavelength dispersive X-ray fluorescence spectrometer (Bruker, Germany), which usage has been approved by the US Environmental Protection Agency (U.S. EPA; Chow and Watson, 1994). Additional information can be found in Wang *et al.* (2018).

Coefficients of Divergence (CDs)

CDs, as a self-normalizing parameter, were evaluated to understand the differences and similarities in the concentrations observed in the five sampling sites. This parameter was computed as follows (Park and Kim, 2004; Kuo *et al.*, 2014):

$$CD = \sqrt{\frac{1}{m}\sum_{i=1}^{m}\left(\frac{x_{ij}-x_{ik}}{x_{ij}+x_{ik}}\right)^2} \quad (1)$$

where x_{ij} and x_{ik} are the concentrations of chemical component i in sites j and k, respectively, and m is the number of measurement days. In the previous analysis (Contini *et al.*, 2012), the values of these coefficients can be used to infer the spatial homogeneity of $PM_{2.5}$ composition in different sites. If the CDs approach 0 or lower than 0.2, then the two sampling sites have a relatively homogeneous spatial distribution. Meanwhile, if the CDs approach 1, then these two sampling sites are different.

Back Trajectory Analysis

The 48-hour backward air trajectories in the five sampling sites with 4-hour intervals were calculated by using the HYSPLIT-4 model (US National Oceanic and Air Administration Air Resources Laboratory). The altitude was set to 500 m. Meteorological data from the Global Data Assimilation System were also used in the calculation.

PSCF Model

The PSCF model was used to ascertain the potential source regions (Liu *et al.*, 2018). The pollution value of $PM_{2.5}$ was 75 μg m^{-3}, the study domain ranged from 31°N to 38°N and from 102°E to 115°E, and the resolution of the grid cells was 0.3° × 0.3°. Other detailed descriptions can be found in the Supplemental Materials.

PMF Model

The PMF model, which is widely applied as a receptor model (Paatero and Tapper, 1994; Paatero, 1997), divides the sample data matrix into two (factor contribution (G) and feature profile (F)) to quantitatively identify the source of contaminants. The factor contributions and profiles were derived via the PMF model by minimizing the objective function Q. The identification of data matrix X, objective function Q, and uncertainty is further described in the Supplemental Materials.

In this study, the program was run several times to find the smallest value of Q_{expect} and to reduce the observed value of residual error matrix E as much as possible in order to ensure that the simulation results show a good correlation with the observations. The stability of a PMF solution was estimated based on the bootstrap (BS), displacement (DISP), and BS-DISP results. After running the program several times, the number of sources was set from four to nine, and the results of six sources were selected due to their adequate fit to the measurement data and their physical meaning (more details can be found in Table 2). These results were constrained with dQ_{robust} of 0.6%, and Fpeak = 0.0 produced the most physically reasonable source profiles.

Health Risk Assessment

The United States Environmental Protection Agency (U.S. EPA) developed an assessment model for estimating the carcinogenic and non-carcinogenic health risks of being exposed to particles. This study was based on the following assumptions. The target subjects were divided into two groups (Jiang *et al.*, 2018e), namely, children < 15 years and adults. The non-carcinogenic risks from V, Cu, As,

Table 2. Summary of PMF and error estimation diagnostics from four to nine factors.

	4 factors	5 factors	6 factors	7 factors	8 factors	9 factors
Q_{except}	4196	3936	3676	3416	3156	2896
Q_{Robust}	33711	27756	22706	18723	15590	13067
Q_{True}	45329	34431	26521	21324	17054	14003
Q_{true}/Q_{exp}	10.87	8.81	7.27	6.30	5.46	4.89
$Q_{robust}/Q_{expected}$	8.03	7.05	6.18	5.48	4.94	4.51
DISP%dQ	–0.071	0	0	0	0	0
DISP swaps	0	0	0	0	0	0
Factor with BS mapping < 80%	factor 1, 45%	factor 4, 75%	all factors > 80%	all factors > 80%	factor 1, 75%	factor 9, 40%

Mn, Zn, Pb, and Ni and the carcinogenic risks from As, Pb, and Ni for children and adults were calculated from three exposure pathways, including inhalation, ingestion, and dermal absorption. The exposure and risk assessments are described in Jiang *et al.* (2018e).

To evaluate the human health risks of these pollutants, In addition, different sources of the same element have different levels of toxicity. the results of the PMF model were combined with those of the risk assessment model. The non-carcinogenic risk index hazard quotient (HQ) and carcinogenic risk index (CR) of the pollution sources were computed as

$$HQ\,or\,CR = \sum_{i=1}^{n} X_i \times HQ_i\ or \sum_{i=1}^{n} X_i \times CR_i \quad (2)$$

where X_i denotes the contribution of each pollution source derived from the PMF model to the i element in the entire sampling period, while HQ_i and CR_i are the i element risk values calculated by the risk assessment model described above.

RESULTS AND DISCUSSION

$PM_{2.5}$ Mass Concentrations

The annual mean $PM_{2.5}$ concentration in the five sampling sites in 2016 was 119 μg m^{-3} (Fig. 2 and Table S1), which was 2.4 times higher than the annual concentration standard (35 μg m^{-3}) proposed by the Chinese National Ambient Air Quality Standard (NAAQS). Although lower than those values in 2013 (191 μg m^{-3}), 2014 (185 μg m^{-3}), and 2015 (150 μg m^{-3}; Jiang *et al.*, 2018c), the 119 μg m^{-3} concentration exceeded those that were in the Yangtze River Delta (60 μg m^{-3}; Feng *et al.*, 2015), Taiwan (24 μg m^{-3}; Hsu *et al.*, 2017), and Lecce (Southern Italy, 19 μg m^{-3}; Cesari *et al.*, 2017), thereby underscoring the severity of $PM_{2.5}$ pollution in Zhengzhou. The daily $PM_{2.5}$ concentration in the city varied from 18 μg m^{-3} to 666 μg m^{-3}, over half (60.5%) of which exceeded the daily standard of the Chinese NAAQS (75 μg m^{-3}). This proportion can even reach as high as 98% during winter. Meanwhile, the seasonal average $PM_{2.5}$ concentration demonstrated the following decreasing order: 221 ± 126 μg m^{-3} (62 μg m^{-3} to 666 μg m^{-3}) in winter, 98 ± 34 μg m^{-3} (39 m^{-3} to 200 μg m^{-3}) in spring, 88 ± 39 μg m^{-3} (37 μg m^{-3} to 218 μg m^{-3}) in autumn, and 47 ± 16 μg m^{-3} (18 μg m^{-3} to 86 μg m^{-3}) in summer. The main factors that influence the $PM_{2.5}$ concentration included the characteristics and loads of pollution sources, particulate characteristics, and meteorological factors. The low $PM_{2.5}$ concentrations during summer can be ascribed to the initiative of the Zhengzhou Municipal Environmental Protection Bureau to reduce the amount of pollutant emissions (ZMPB, 2016). Meanwhile, the high $PM_{2.5}$ concentrations in winter may be ascribed to the increased amounts of emissions, such as those from coal-fired heating, and adverse meteorological conditions, such as frequent winter temperature inversion and relatively stable atmospheric conditions (Liu *et al.*, 2017).

The $PM_{2.5}$ concentrations of the five sampling sites are presented in Table S1. The results showed that the highest annual mean $PM_{2.5}$ concentrations were observed in the urban site of SSQ (137 ± 113 μg m^{-3}) and the traffic site of HKG (131 ± 91 μg m^{-3}), followed by the rural site of ZM (112 ± 112 μg m^{-3}) and the industrial site of XM (111 ± 85 μg m^{-3}) and the lowest annual mean $PM_{2.5}$ concentration (104 ± 82 μg m^{-3}) was in the scenic site of DF. The differences in the $PM_{2.5}$ concentrations of the five sampling sites were calculated based on CDs (Fig. 3) SSQ and HKG have the lowest CD values, possibly because they have a large amount of traveling vehicles and airplanes, thereby implying that vehicle emission may have an important role in increasing the $PM_{2.5}$ concentration. Relatively few emission sources were reported near DF, which is a scenic area. A lag time in the $PM_{2.5}$ concentration peak was also in each sampling site as shown in Fig. 2. Specifically, the concentration peak appeared earliest in ZM and latest in DF, which may be explained by the heavy pollution days transfer from the northeast.

Characteristics of Chemical Species in $PM_{2.5}$

WSIIs Analysis

Consistent with previous studies (Squizzato *et al.*, 2013; Yin *et al.*, 2014; Meng *et al.*, 2016), this paper identified nine WSIIs that comprise $PM_{2.5}$ (Table S1). These WSIIs accounted for 47.7% of the annual $PM_{2.5}$ mass concentration and 47.9%, 42.3%, 51.2%, and 49.4% of the $PM_{2.5}$ mass concentrations in winter, spring, summer, and autumn, respectively. Compared with other cities such as Wuhan (43.7% to 41.8%; Zhang *et al.*, 2015) and Shanghai (32.0%; Wang *et al.*, 2006b), Zhengzhou has a higher ratio of WSIIs/$PM_{2.5}$, thereby indicating that WSIIs are important constituents of the atmospheric $PM_{2.5}$ pollutants in the city.

The annual WSIIs concentrations in Zhengzhou demonstrate the following decreasing order: NO_3^- (20.4 ± 24.2 μg m^{-3}) > SO_4^{2-} (17.7 ± 17.6 μg m^{-3}) > NH_4^+ (13.2 ± 11.4 μg m^{-3}) >

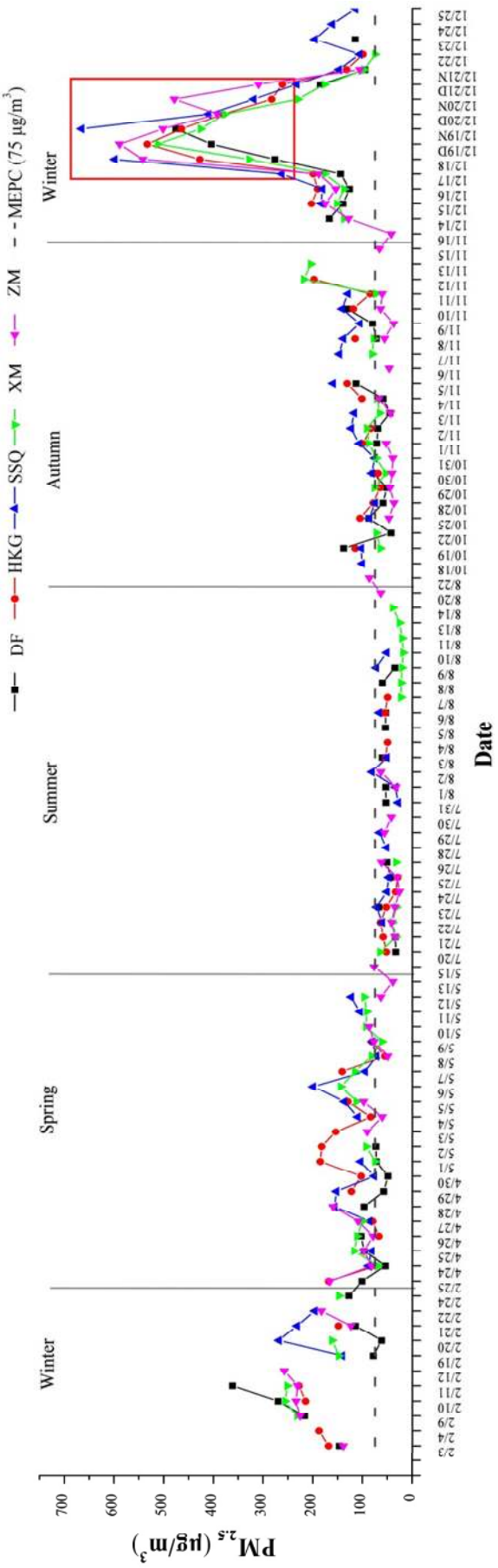

Fig. 2. Temporal variations of $PM_{2.5}$ concentrations in five sampling sites in Zhengzhou, MEPC: Ministry of Environmental Protection of China. (D: daytime; N: night)

Cl^- (2.6 ± 3.5 μg m^{-3}) > Ca^{2+} (1.5 ± 1.5 μg m^{-3}) > K^+ (1.4 ± 2.0 μg m^{-3}) > Na^+ (0.4 ± 0.3 μg m^{-3}) > F^- (0.2 ± 0.2 μg m^{-3}) > Mg^{2+} (0.1 ± 0.1 μg m^{-3}). Secondary inorganic aerosols (SIAs) (NH_4^+, SO_4^{2-}, and NO_3^-) were the major components of these WSIIs and accounted for an average of 88.4% of the total ions in the five sampling sites across all four seasons. This percentage is nearly the same as those reported in Beijing (86.3%, Deng *et al.* 2011), Handan (87.0%, Meng *et al.*, 2016), and Hefei (82.0%, Deng *et al.*, 2016).

The seasonal variations in the WSIIs are shown in Table S1. The seasonal concentrations of SO_4^{2-} and Cl^- were highest in winter, which may be related to coal-burning heating for residents in North China in this season. In addition, the stable atmospheric structure in winter is not conducive to the diffusion of pollutants. NO_3^- had the highest contribution in winter due to the combined action of photochemical and heterogeneous reactions, NO_x emissions, and gas-aerosol equilibrium (Zhang *et al.*, 2013). NH_4^+ concentration was larger in winter because poor dispersion and the lower removal rate in this season. However, the highest concentrations of Mg^{2+} and Ca^{2+} were observed in spring, which may be ascribed to the dry winds blowing in the area during this season. By contrast, the concentration of all WSIIs were lower in summer, because the height of the planetary boundary layer is higher in summer, which is contributes to the diffusion of pollutants (Yang *et al.*, 2015). In addition, the lowest concentration of NO_3^- in summer may be related to the loss of nitrate particles to the gaseous phase due to the high temperature in summer (Diapouli *et al.*, 2017). Meanwhile, the CD results showed that Na^+, K^+, NO_3^-, and SO_4^{2-} followed a relatively homogeneous spatial distribution while all the other WSIIs demonstrated varying characteristics across the five sampling sites, especially in DF (Fig. 3).

The equivalent concentrations of cations (CE) and anions (AE) were computed as

$$AE = \frac{SO_4^{2-}}{48} + \frac{NO_3^-}{62} + \frac{Cl^-}{35.5} + \frac{F^-}{19} \quad \text{and} \tag{3}$$

$$CE = \frac{Na^+}{23} + \frac{NH_4^+}{18} + \frac{K^+}{39} + \frac{Mg^{2+}}{12} + \frac{Ca^{2+}}{20} \tag{4}$$

Fig. 4 presents the scatter diagram of AE versus CE in all four seasons. The samples collected in each season were above the 1:1 (CE:AE) line, thereby suggesting that the cations were not completely neutralized by anions and hence showed an alkaline property (Meng *et al.*, 2016). This observation can also be attributed to the existence of other anions, such as CO_3^{2-} and HCO_3^-, which were not analyzed in this study. Meanwhile, the sample collected for winter, specifically the sample with a higher concentration, was below the 1:1 (CE:AE) line and showed an acidic property, thereby suggesting that the ion composition of $PM_{2.5}$ in winter was more complex than the compositions of $PM_{2.5}$ in other seasons. This finding explains why the most serious level of air pollution is often observed during winter (Huang *et al.*, 2016). Fig. 5 presents the scatter plots of (a) NH_4^+

	HKG-DF	SSQ-DF	ZMD-DF	XM-DF	ZM-XM	ZM-SSQ	HKG-ZM	XM-SSQ	HKG-XM	HKG-SSQ	
$PM_{2.5}$	0.20	0.25	0.19	0.19	0.16	0.25	0.18	0.22	0.18	0.13	$PM_{2.5}$
OC	0.19	0.25	0.27	0.23	0.22	0.31	0.20	0.31	0.20	0.16	OC
EC	0.36	0.36	0.33	0.32	0.26	0.33	0.25	0.26	0.23	0.21	EC
Cl⁻	0.49	0.43	0.41	0.45	0.27	0.30	0.26	0.31	0.30	0.21	Cl⁻
Na^+	0.26	0.29	0.23	0.29	0.34	0.26	0.21	0.29	0.27	0.18	Na^+
K^+	0.22	0.27	0.21	0.23	0.27	0.21	0.17	0.27	0.20	0.18	K^+
NO3-	0.33	0.34	0.31	0.32	0.20	0.23	0.18	0.27	0.17	0.17	NO3-
SO_4^{2-}	0.23	0.26	0.28	0.23	0.20	0.16	0.18	0.19	0.13	0.14	SO_4^{2-}
F^-	0.45	0.36	0.43	0.52	0.67	0.47	0.52	0.48	0.48	0.40	F^-
Ca^{2+}	0.46	0.46	0.35	0.35	0.40	0.46	0.40	0.32	0.32	0.29	Ca^{2+}
Mg^{2+}	0.36	0.37	0.34	0.29	0.36	0.42	0.36	0.28	0.26	0.24	Mg^{2+}
Al	0.39	0.42	0.35	0.38	0.35	0.44	0.40	0.26	0.27	0.26	Al
Si	0.39	0.40	0.35	0.31	0.29	0.42	0.38	0.27	0.31	0.26	Si
Ti	0.42	0.45	0.32	0.37	0.31	0.44	0.33	0.29	0.30	0.30	Ti
Ni	0.58	0.53	0.66	0.55	0.60	0.56	0.64	0.46	0.55	0.52	Ni
Cu	0.41	0.50	0.37	0.44	0.38	0.35	0.27	0.51	0.38	0.33	Cu
Zn	0.75	0.77	0.76	0.73	0.35	0.25	0.20	0.34	0.39	0.22	Zn
Ga	0.52	0.50	0.50	0.52	0.48	0.41	0.41	0.38	0.38	0.36	Ga
As	0.60	0.65	0.55	0.64	0.42	0.44	0.43	0.36	0.39	0.39	As
Se	0.52	0.59	0.54	0.49	0.39	0.33	0.30	0.46	0.29	0.40	Se
Sr	0.44	0.55	0.42	0.28	0.49	0.51	0.54	0.46	0.41	0.50	Sr
Cr	0.69	0.67	0.66	0.72	0.46	0.54	0.44	0.53	0.47	0.50	Cr
Ba	0.62	0.64	0.59	0.62	0.49	0.56	0.40	0.42	0.57	0.52	Ba
Sb	0.39	0.49	0.35	0.43	0.35	0.33	0.29	0.31	0.34	0.31	Sb
V	0.25	0.29	0.26	0.28	0.44	0.29	0.33	0.22	0.28	0.24	V
Pb	0.27	0.31	0.24	0.16	0.21	0.19	0.17	0.23	0.26	0.19	Pb
Mn	0.40	0.43	0.25	0.27	0.17	0.35	0.26	0.27	0.29	0.22	Mn
Fe	0.40	0.45	0.30	0.27	0.23	0.43	0.35	0.32	0.33	0.27	Fe
	HKG-DF	SSQ-DF	ZM-DF	XM-DF	ZM-XM	ZM-SSQ	HKG-ZM	XM-SSQ	HKG-XM	HKG-SSQ	

Fig. 3. CDs of different chemical species for five sites in Zhengzhou.

versus SO_4^{2-} and (b) NH_4^+ versus [SO_4^{2-} + NO_3^-]. This figure further illustrates how NH_4^+ relates to the major acidic ions, including SO_4^{2-} and NO_3^-. Fig. 5(a) shows that SO_4^{2-} can be fairly sufficient to be neutralized by NH_4^+; therefore, $(NH_4)_2SO_4$ is the existence form of SO_4^{2-}. Fig. 5(b) shows that all samples are positioned around the 1:1 line, thereby indicating that the $PM_{2.5}$ samples occupy a sufficient NH_4^+ to neutralize SO_4^{2-} and NO_3^- to $(NH_4)_2SO_4$ and NH_4NO_3, respectively. Given that $(NH_4)_2SO_4$ is less volatile than NH_4NO_3, the former can be formed preferentially. The results of a comparative analysis show that a high $PM_{2.5}$ concentration, especially above 300 μg m^{-3}, significantly deviates from the 1:1 line, which in turn may suggest that NH_4^+ is not enough to cancel out SO_4^{2-} and NO_3^- simultaneously. Therefore, NO_3^- exists in the form of NH_4NO_3 and HNO_3 (Zhang *et al.*, 2013; Meng *et al.*, 2016).

The mass ratio of NO_3^-/SO_4^{2-} can be used to indicate the relative contribution of fixed and mobile sources in the atmosphere (Yao *et al.*, 2002; Xiao and Liu, 2004). According to Arimoto *et al.* (1996), a high NO_3^-/SO_4^{2-} ratio indicates that the contribution of mobile sources is more significant than that of stationary sources. In this study, the average annual ratio of NO_3^-/SO_4^{2-} in Zhengzhou was 1.0 (Table S2). Meanwhile, the mass ratio in the city was greater than the NO_3^-/SO_4^{2-} ratio (0.63) in Heze from 2015 to 2016 (Liu *et al.*, 2017) and less than the mass ratio (1.10) in Hefei from 2012 to 2013 (Deng *et al.*, 2016). The high NO_3^-/SO_4^{2-} mass ratio in Zhengzhou may be attributed to the high traffic density in the city. The average NO_3^-/SO_4^{2-} mass ratio also showed seasonal variations in the following decreasing order: winter (1.3) = autumn (1.3) > spring (1.0) > summer (0.4). The lowest mass ratio of NO_3^-/SO_4^{2-} was during summer probably because the stability of NH_4NO_3 was reduced under the high temperatures during summer and the rate of NO_3^- formation decreased. Meanwhile, the high mass ratios of NO_3^-/SO_4^{2-} in winter and autumn may be attributed to the fact that the low temperatures increased the rate of NO_3^- formation (Deng *et al.*, 2016).

Carbonaceous Material Analysis

The average annual concentration values of OC and EC in Zhengzhou were 15.4 and 2.1 μg m^{-3}, which accounted for 12.6% and 1.8% of $PM_{2.5}$, respectively (Table S1). This level was close to the values of carbon aerosols observed at regional sites throughout China (16.1 ± 5.2 μg m^{-3} for OC and 3.6 ± 0.9 μg m^{-3} for EC; Zhang *et al.*, 2008).

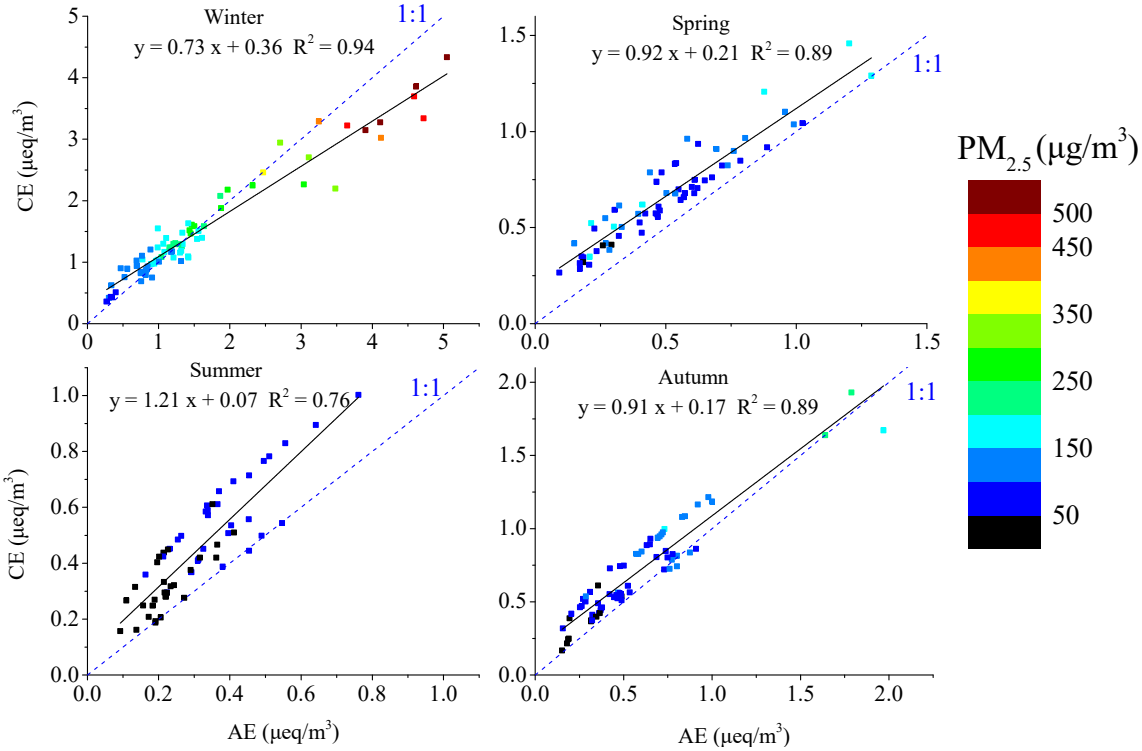

Fig. 4. Scatter plots of AE versus CE in four seasons in Zhengzhou. Different colors correspond to different concentrations of $PM_{2.5}$.

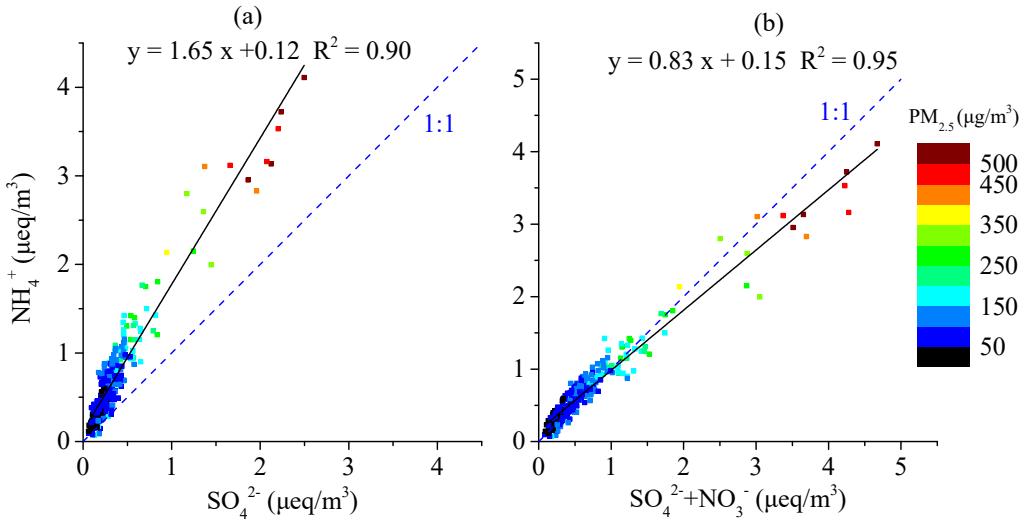

Fig. 5. Scatter plots of (a) NH_4^+ versus SO_4^{2-} and (b) NH_4^+ versus $[SO_4^{2-} + NO_3^-]$ in Zhengzhou. Different colors correspond to different concentrations of $PM_{2.5}$.

Similar to $PM_{2.5}$, the seasonal changes of OC and EC were reduced in the following order: winter (30.8 μg m^{-3} and 4.0 μg m^{-3}) > autumn (10.9 μg m^{-3} and 1.6 μg m^{-3}) ≈ spring (10.8 μg m^{-3} and 1.7 μg m^{-3}) > summer (5.8 μg m^{-3} and 0.7 μg m^{-3}). The OC and EC concentrations in SSQ (18.2 μg m^{-3} and 2.2 μg m^{-3}) and HKG (16.6 μg m^{-3} and 2.7 μg m^{-3}) exceeded those in ZM (15.4 μg m^{-3} and 2.2 μg m^{-3}), XM (13.0 μg m^{-3} and 2.0 μg m^{-3}), and DF (13.9 μg m^{-3} and 1.5 μg m^{-3}) mainly due to the influence of vehicle emissions. The coefficient of correlation (R^2) between OC and EC in autumn exceeded those in other seasons (Fig. S1), thereby suggesting that OC and EC may come from similar sources in autumn to a certain extent. In sum, OC and EC demonstrate various characteristics in different sampling sites in different seasons.

OC comprises secondary organic carbon (SOC) and primary organic carbon (POC). Previous studies (Turpin and Huntzicker, 1995; Zhang *et al.*, 2007; Zhang *et al.*, 2013) have demonstrated the possible existence of SOC when the OC/EC ratio exceeds 2.0 to 2.2. In this study, the

average annual OC/EC ratio was 8.3, which slightly varied across seasons (9.9, 8.7, 7.6, and 7.0 in winter, summer, autumn, and spring, respectively). These variations may indicate the presence of SOC in the atmosphere (Zhang *et al.*, 2007; Zhang *et al.*, 2013). The contribution of SOC to the formation of secondary organic aerosols can be estimated by calculating SOC as follows (Yuan *et al.*, 2005):

$$SOC = OC - POC = OC - EC \times \left(\frac{OC}{EC}\right)_{min}, \quad (5)$$

where SOC (μg m^{-3}) and OC (μg m^{-3}) are the concentrations of SOC and OC, respectively, and $(OC/EC)_{min}$ represents the minimum OC/EC ratio in each site across different seasons throughout the sampling period.

In this study, SOC concentrations followed a decreasing order: winter (13.0 ± 15.0 μg m^{-3}) > autumn (5.1 ± 3.9 μg m^{-3}) > spring (4.2 ± 3.2 μg m^{-3}) > summer (2.2 ± 1.7 μg m^{-3}). The SOC/OC and SOC/$PM_{2.5}$ ratios were obviously high during autumn, which may be explained by the contributions of various sources and the influence of meteorological conditions on the formation of SOC. SOC significantly contributed to the OC and $PM_{2.5}$ mass in SSQ, thereby suggesting that the unique topography around the urban center was prone to the accumulation of atmospheric pollutants and the formation of SOC (Li *et al.*, 2016).

Elements

A total of 21 elements (Zn, Na, Ca, Al, Si, K, Mg, Ni, Ti, V, Cu, As, Fe, Mn, Cr, Pb, Ga, Se, Sr, Sb, and Ba) were detected in $PM_{2.5}$ and accounted for 9.6% of the $PM_{2.5}$ studied in this paper (Table S3). Crustal elements (i.e., Fe, Si, K, Ti, Ca, Mn, Mg and Al) dominated the tested elements of $PM_{2.5}$ and accounted for 93.1% of all tested elements in Zhengzhou. High crustal elements concentration was observed in spring probably because of the frequent dust weather events during this season (Geng*et al.*, 2013). The CD values for these elements are presented in Fig. 3. The pollution characteristics of DF, especially the elements from anthropogenic resources (e.g., Zn, Cr, Ba, and As) obviously differed from those of other sites. The characteristics of crustal elements (Ca, Mg, Al, Si, and Ti) in ZM were different from those in SSQ because ZM is an agriculture area (Liu *et al.*, 2017) whereas SSQ is an urban area (Aldabe *et al.*, 2011). SSQ and HKG demonstrated similar pollution characteristics. In general, the differences in the chemical species analyzed in the five sampling sites were significant.

The concentrations of crustal elements in the $PM_{2.5}$ collected from the five sampling sites followed a decreasing order: SSQ (13.0 ± 12.3 μg m^{-3}), HKG (12.9 ± 14.2 μg m^{-3}), XM (10.1 ± 9.0 μg m^{-3}), ZM (5.8 ± 3.6 μg m^{-3}), and DF (5.7 ± 5.7 μg m^{-3}) (Table S3). The high concentrations of crustal elements in HKG and SSQ might be attributed to vehicles sweeping a large amount of dust on the road, while the low concentrations in ZM and DF could be attributed to the scarcity of soil sources around these rural and scenic areas (Table 1). Although the elements (i.e., Zn, V, Sb, Cr, Sr, Ni, Se, As, Ga, Cu, Pb, and Ba) accounted for only 6.9% of the measured elements in Zhengzhou, they are all deemed toxic to humans. The annual concentrations of As in all sites, especially in SSQ (17.8 ± 15.7 ng m^{-3}), greatly exceeded the Chinese NAAQS limit of 6 ng m^{-3}. By contrast, the average annual concentrations of V, Pb, Mn, and Ni were below the limits set by (World Health Organization) WHO (25, 500, 150, and 1000 ng m^{-3} for Ni, Pb, Mn, and V, respectively).

The influence of human activities and the natural background of those particles associated with the elements were determined by analyzing the enrichment factor (EF) (Zheng *et al.*, 2004; Betha *et al.*, 2014; Jiang *et al.*, 2017), which was calculated by using Eq. (6) (Taylor *et al.*, 1964; Hsu *et al.*, 2010). In the following, Al was taken as the reference element and the concentration of elements in the surface soil of China was taken as the crust elements concentration value in the crust (Hsu *et al.*, 2016).

$$EF_x = \frac{(E/Al)_{Particulates}}{(E/Al)_{Crust}}, \quad (6)$$

where $(E/Al)_{Particulates}$ and $(E/Al)_{Crust}$ are the concentration ratios of the target metal to the reference element Al in the samples and the continental crust, respectively. In this study, an EF value of below 10 indicates that the element mainly comes from natural sources, while an EF value of above 10 indicates that the element may come from human sources (Xu *et al.*, 2013; Zhang *et al.*, 2015).

The EF values of each element of $PM_{2.5}$ collected from the five sampling sites across different seasons are presented in Figs. S2–S3, which show that Si, K, Mg, Mn, Ti, Fe, Cr, Ba, V, Ni, and Sr have annual average EF values of lower than 10. Therefore, these elements mainly come from crustal sources (Xu *et al.*, 2013). Ca, Cu, As, Ga, Na, Zn, Pb, and Sb were enriched with annual average EF values of above 10, thereby suggesting that these elements are influenced by human sources (Zhang *et al.*, 2015). Zn, Pb, and Sb (with annual average EF > 100) were anomalously enriched. Generally, many metals (i.e., Na, K, Mg, Pb, Ba, As, and Sr) showed high EF values during winter, while some metals (Mn, Cu, Cr, V, Ni, Ga, and Sb) showed high EF values during summer. Fig. S2 shows that the EF values of many metals, except for Si, Ca, Fe, Ni, and Ga, are high in ZM.

Chemical Mass Closure

An $PM_{2.5}$ chemical mass closure was structured in the five sampling sites in consideration of SIAs, dust, EC, organic matter (OM), WSIIs (F^-, K^+, Cl^-, Mg^{2+}, Na^+, and Ca^{2+}), and elements, except for crustal elements (Ca, Al, Ti, Fe, and Si). In this study, OM was estimated as OC multiplied by 1.8 in Chinese cities (Wang *et al.*, 2006b; Tao *et al.*, 2014).

The dust was calculated by the crustal species as

$$[Dust] = 1.94 \times [Ti] + 2.20 \times [Al] + 2.42 \times [Fe] + 1.63 \times [Ca] + 2.49 \times [Si], \quad (7)$$

The chemical composition that was reconstructed based

on the seasonal and annual average concentrations of $PM_{2.5}$ in the five sampling sites is shown in Fig. 6 and Table S1. SIAs had the highest proportion across all five sampling sites and accounted for more than 40.0% of the annual $PM_{2.5}$ concentration in Zhengzhou, with the largest and smallest values in DF (46.3%) and SSQ (40.0%), respectively. OM showed minimal differences across all sampling sites (large in SSQ and DF (24.0%) and small in XM (19.8%), with an average of 22.7%). By contrast, dust exhibited significant differences across all sites (19.3%, 12.7%, 14.0%, 18.9%, 10.6%, and 15.1% in HKG, ZM, XM, SSQ, and DF, respectively). The ratios of EC, WSIIs, and elements (except for crustal elements) in $PM_{2.5}$ were 1.8%, 4.8%, and 0.6% on average, respectively. Obvious seasonal changes were also reported in dust (significantly larger in spring and smaller in winter and summer), OM (larger in winter and smaller in spring), SIAs (larger in summer and smaller in spring), and elements (slightly larger in summer and autumn and smaller in winter and spring).

Source Apportionment by PMF

The PMF model was used to determine the contributions of sources by using the datasets collected from the five sampling sites as input data. PMF analysis was performed on 23 species, including OC, EC, Na, NH_4^+, SO_4^{2-}, NO_3^-, Al, Ca, V, Mg, Si, Zn, Cl^-, K, As, Se, Ti, Ni, Cu, Pb, Cr, Mn, and Fe, all of which were classified as "strong" variables (Jiang *et al.*, 2018e). The data for these species satisfy the requirements for PMF 5.0 input data analysis (U.S. EPA, 2014). Six primary sources of $PM_{2.5}$, namely, secondary aerosol, coal combustion, dust, biomass combustion, vehicular traffic, and industry, were eventually identified (Fig. 7).

The first factor was related to dust with high abundance of Na, Mn, Al, Si, Ti, Mg, Fe, and Ca in $PM_{2.5}$ than other species. Soil and road dusts are major species in the atmosphere that mainly comprise Ca, Fe, Al, Mg, K, and other elements (Lough *et al.*, 2005; Jiang *et al.*, 2018a). Dust has an annual contribution of 15.1% to the $PM_{2.5}$ pollution in Zhengzhou (Table 3); this percentage was lower than those in Lanzhou in 2014 (21.8%; Wang *et al.*, 2016) and Heze between 2015 and 2016 (19.2%; Liu *et al.*, 2017) but was higher than those in Beijing (8.6%), Tianjin (11.7%) and Shijiazhuang (8.5%) between 2014 and 2015 (Huang *et al.*, 2017). Similar to the findings of Zhang *et al.* (2013) and Chen *et al.* (2017), the contributions of dust in the $PM_{2.5}$ pollution in Zhengzhou showed an obvious seasonal distribution. For instance, a higher dust concentration was observed in spring (21.3% ± 18.3%), which can be ascribed to the frequent sandstorms in Zhengzhou during this season (Jiang *et al.*, 2018e). A significant difference was also observed across all five sampling sites. Specifically, high contributions were observed in SSQ (18.2%) and HKG (17.5%), which echoed the results for chemical mass closure.

The second factor was categorized as vehicular traffic, which is characterized by OC, EC, NO_3^-, V, Ni, Cu, Zn, Pb, and Mn, all of which are often considered tracers of vehicular traffic (Viana *et al.*, 2006; Charlesworth *et al.*, 2011). Cu is related to break wear, and Ni is produced by the combustion of oil (Garg *et al.*, 2000). Vehicular traffic accounted for 17.3% of the $PM_{2.5}$ mass in Zhengzhou and did not show any obvious seasonal variation probably due to the annual uniform emission load. Compared with other cities in China, the contributions of vehicular traffic to air pollution in Zhengzhou are relatively high, only less than Beijing between 2014 and 2015 (24.9%; Huang *et al.*, 2017)

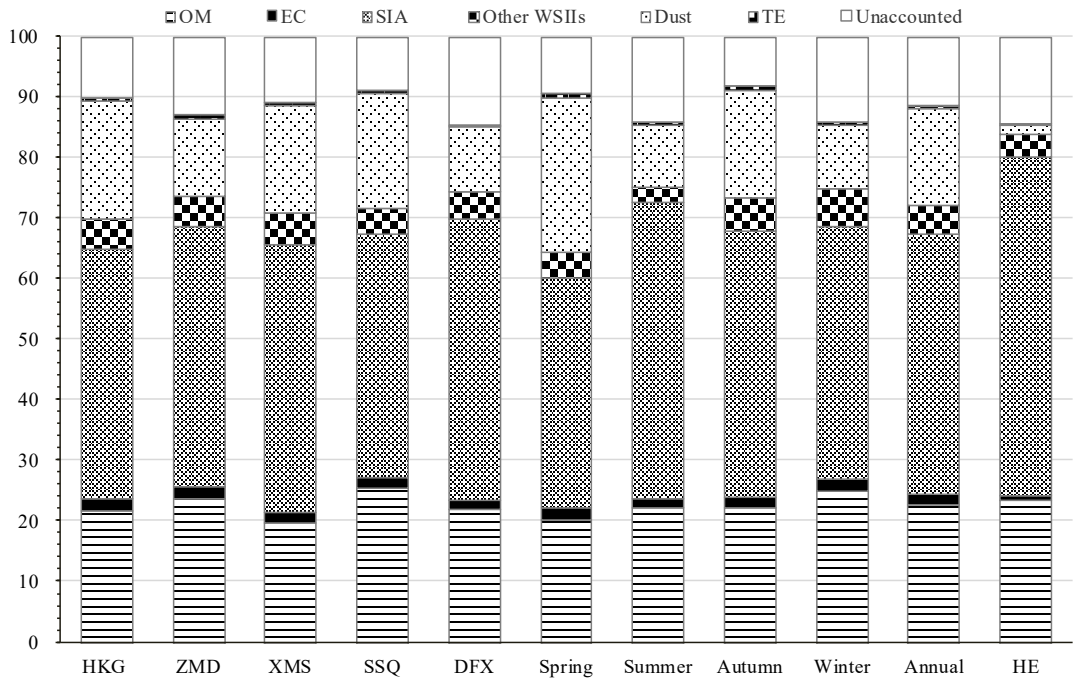

Fig. 6. Average compositional fractions (%) of $PM_{2.5}$ in five sites and heavy pollution days (December 18–20, 2016) in Zhengzhou. (TE: total elements)

Table 3. Contributions of $PM_{2.5}$ in five sampling sites in Zhengzhou and comparison with other city in China.

Year	%		Coal combustion	Biomass combustion	Vehicular traffic	Industrial	Dust	Secondary aerosol	Others	
2016	HKG		15.9 ± 13.2	6.6 ± 3.8	18.6 ± 11.0	8.2 ± 3.4	17.5 ± 16.9	33.2 ± 23.9	-	This study
	ZM		18.4 ± 17.8	10.7 ± 6.1	15.8 ± 13.1	5.4 ± 3.0	14.8 ± 12.7	35.0 ± 21.2	-	
	XM		20.4 ± 14.5	7.6 ± 5.3	13.4 ± 15.0	11.4 ± 11.1	13.7 ± 14.8	33.4 ± 21.8	-	
	SSQ		16.5 ± 5.4	5.7 ± 3.6	22.1 ± 15.5	4.2 ± 2.4	18.2 ± 15.5	33.3 ± 18.1	-	
	DF		16.3 ± 10.8	7.3 ± 5.1	16.5 ± 9.8	7.2 ± 6.9	10.7 ± 9.1	42.0 ± 21.0	-	
	Winter		21.1 ± 17.0	8.1 ± 4.8	16.9 ± 13.2	7.8 ± 7.7	11.1 ± 13.6	35.0 ± 26.7	-	
	Spring		15.1 ± 9.7	6.7 ± 3.8	18.6 ± 12.2	7.1 ± 6.9	21.3 ± 18.3	31.2 ± 17.0	-	
	Summer		17.5 ± 15.7	5.3 ± 4.6	17.4 ± 17.8	5.8 ± 4.9	12.1 ± 10.3	41.9 ± 19.7	-	
	Auturmn		16.5 ± 9.0	9.6 ± 6.2	16.2 ± 10.6	8.1 ± 8.3	15.8 ± 11.8	33.7 ± 16.0	-	
	Annual		17.6 ± 13.4	7.7 ± 5.2	17.3 ± 13.5	7.3 ± 7.2	15.1 ± 14.4	35.1 ± 21.1	-	
	HE (Dec. 18–20, 2016)		28.3 ± 12.2	8.4 ± 1.6	14.0 ± 5.3	11.8 ± 5.0	4.6 ± 4.0	57.3 ± 13.0	-	
2014–2015	Beijing		5.6	4.5	24.9	3.2	8.6	40.5	12.7	Huang *et al.*, 2017
	Tianjin		12.4	5.3	15.2	11.7	11.7	29.2	14.6	
	Shijiazhuang		15.5	2.8	17.3	7.0	8.5	36.4	12.5	
	Xinglong		0.0	8.9	4.2	2.9	11.1	45.1	27.7	
2015–2016	Heze		17.2	7.0	16.5	3.8	19.2	26.5	9.8	Liu *et al.*, 2017
2009–2010	Beijing	Spring	5	19	5	14	23	34	-	Zhang *et al.*, 2013
		Summer	1	6	4	32	3	54	-	
		Autumn	7	17	4	42	18	13	-	
		Winter	57	7	2	12	16	6	-	
		Annual	18	12	4	25	15	26	-	
2014	Lanzhou		22.3	8.0	21.7	9.6	21.8	16.6	-	Wang *et al.*, 2016
2012–2013	Chongqing	Spring	26.7		7.7	26.3	15.2	24.1	-	Chen *et al.*, 2017
		Summer	19.2		6.3	17.7	4.6	52.2	-	
		Autumn	22.6		11.3	22.2	11.9	32	-	
		Winter	22.4		11	13.9	11.2	41.5	-	
		Annual	22		9.8	19.7	11	37.5	-	

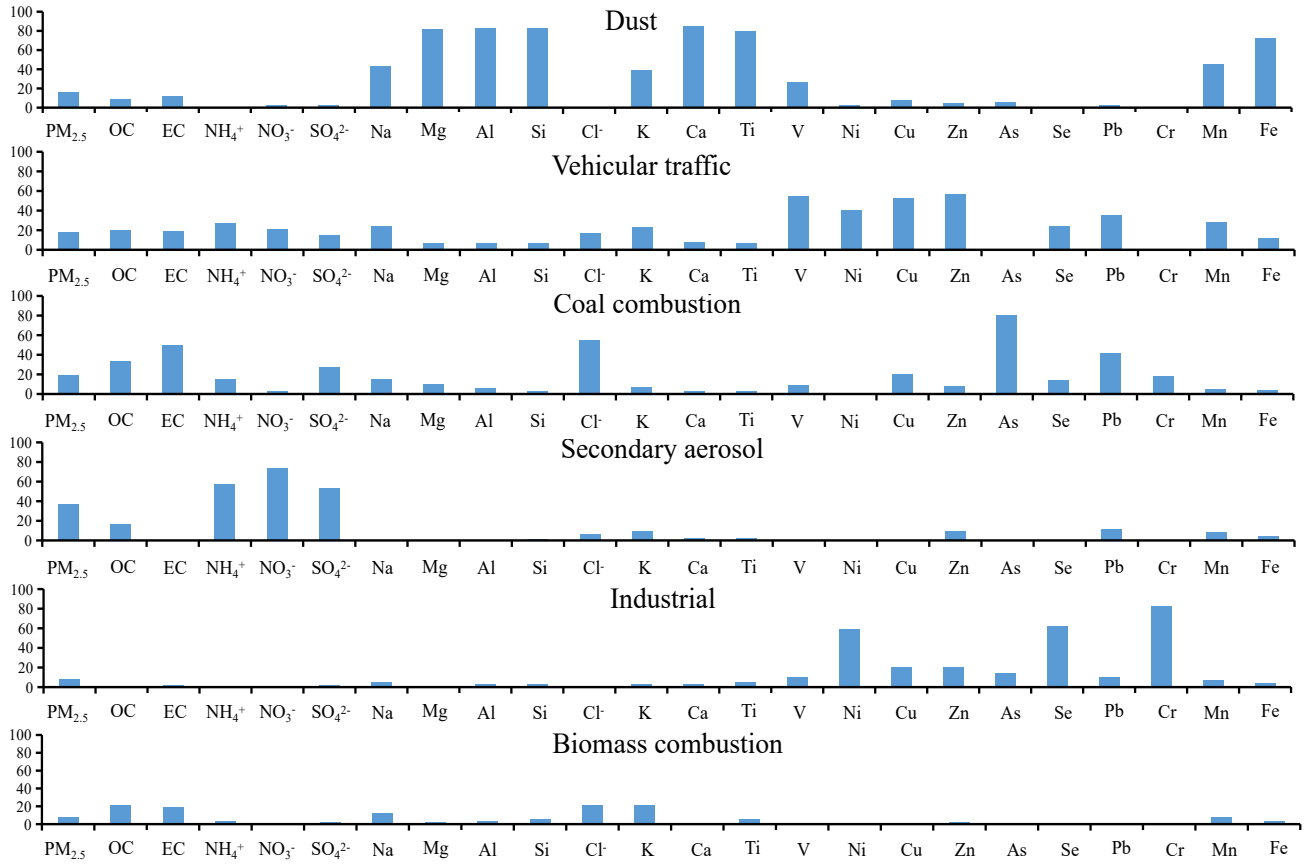

Fig. 7. Source profiles of $PM_{2.5}$ obtained by PMF model analysis in Zhengzhou.

and Lanzhou in 2014 (21.7%; Wang *et al.*, 2016). An obvious difference was also observed among the five sampling sites, with SSQ (22.1%) and HKG (18.6%) showing the largest contributions while XM (13.4%) showing the lowest contributions. These percentages could be ascribed to the characteristics of these sites.

The third factor showed a high loading for Cl^-, OC, Na^+, SO_4^{2-}, As, Na, and Pb, all of which are mainly produced by the burning of coal (Bhangare *et al.*, 2011). This factor accounted for 17.6% of the $PM_{2.5}$ mass in Zhengzhou; this percentage is lower than that in Lanzhou in 2014 (22.3%; Wang *et al.*, 2016) and Chongqing between 2012 and 2013 (22.0%; Chen *et al.*, 2017). The high contributions of coal combustion to the $PM_{2.5}$ pollution in Zhengzhou during winter was closely associated with the high amounts of coal that is burned during this season to generate heat. No obvious seasonal variations were observed in the contributions of this source. Coal combustion showed a significant contribution to the $PM_{2.5}$ pollution in XM (20.4%) but only a small contribution to the $PM_{2.5}$ pollution in HKG (15.9%).

The fourth factor had high loadings on SO_4^{2-}, NO_3^-, and NH_4^+, so it could be identified as the nitrates and sulfates of mixed source of secondary aerosols. The gaseous precursors (NO_x, NH_3, and SO_2) generated by human activities are main sources of secondary ions that are formed in the atmosphere (Perrone *et al.*, 2010). A previous study showed that NO_3^-, SO_4^{2-}, and NH_4^+ are primarily produced by the chemical reactions of particles (Wang *et al.*, 2006a). This source contribute 35.1% to the $PM_{2.5}$ concentrations in Zhengzhou. Although lower than that in Beijing between 2014 and 2015 (40.5%; Huang *et al.*, 2017), this percentage implies a serious degree of secondary aerosol pollution in Zhengzhou. A significant seasonal variation was also observed for this source in the following decreasing order: summer (41.9%) > winter (35.0%) > autumn (33.7%) > spring (31.2%). The intense secondary aerosol reaction reported in summer and winter similar to the results findings of Zhang *et al.* (2013) and Chen *et al.* (2017). The highest contribution of secondary aerosols was reported in DF.

The fifth factor was identified as industry, which was mainly comprised As, V, Pb, Ni, Cr, Se, and Cu, all of which are generally associated with industrial processes (Chan *et al.*, 1997; Turpin and Lim, 2001). Industry contributes around 7.3% to the $PM_{2.5}$ pollution in Zhengzhou; this percentage is obviously lower than that reported in Tianjin between 2014 and 2015 (11.7%; Huang *et al.*, 2017), Beijing between 2009 and 2010 (25.0%; Zhang *et al.*, 2013), and Chongqing between 2012 and 2013 (19.7%; Chen *et al.*, 2017). However, this percentage was higher than in Beijing between 2014 and 2015 (3.2%; Huang *et al.*, 2017) and Heze between 2015 and 2016 (3.8%, Liu *et al.*, 2017). The influence of the environmental supervision conducted by the Zhengzhou Municipal Environmental Protection Bureau between December 18 and 20 in 2016 explains why this source showed the lowest contribution in summer (5.8%) and the largest contribution in autumn (8.1%).

The sixth factor was highly loadings on K, Cl^-, EC, and OC, which could be related to biomass burning (Argyropoulos *et al.*, 2013). Biomass-burning activities, including wildfires in summer, prescribed burning in spring all the way through fall, and heating in winter, occur all year round in Zhengzhou. Biomass combustion contributes to the $PM_{2.5}$ pollution in Zhengzhou during autumn and winter at an average annual rate of 7.7%, which is higher than that reported in Beijing between 2009 and 2010 (12.0%; Zhang *et al.*, 2013). The highest contribution was observed in ZM (10.7%), followed by XM (7.6%) and DF (7.3%).

Compared with the results obtained in 2013 (Geng *et al.*, 2013) where soil dust, vehicle traffic, secondary aerosol, coal combustion, industry, and mixed sources (biomass burning, oil combustion, and incineration) accounted for 26.0%, 10.0%, 24.0%, 23.0%, 4.0%, and 13.0% of the $PM_{2.5}$ pollution in Zhengzhou, respectively, this study reported lower contributions of soil dust and higher contributions of secondary aerosol, vehicle, and industry. These differences underscore some significant changes in the pollution source and emission load. Moreover, the source apportionment results pointed toward the typical characteristics of the five sampling sites. The contributions of vehicle traffic and dust were obviously higher in the urban and traffic sites, thereby indicating the serious degree of vehicle pollution in these areas. The highest contribution of industry was observed in the industrial site, while that of biomass burning was observed in the rural site. These observations were consistent with the characteristics of these areas and can support the government in their decision making.

Back Trajectory Analysis

The results of the backward trajectory analysis on heavily polluted days via the HYSPLIT-4 model are presented in Fig. 8. The air masses from the northeast directions caused the most serious pollution in the entire study area, except in DF. More than 1/3 of the air masses (44.4%, 61.1%, 33.3%, and 38.9% for the ZM, HKG, XM, and SSQ sites, respectively) came from Shandong Province during the heavy pollution period. The air masses originating from Hubei Province were also dominant (27.8% to 66.7%) in these sites, especially in DF with highest value of 66.7%. The $PM_{2.5}$ concentrations were higher in SSQ (537.0 μg m^{-3}), ZM (510.1 μg m^{-3}), and HKG (410.6 μg m^{-3}) compared with the other sites, which may be explained by the accumulation of air pollutants during the long-range transport from Shandong Province and Hubei Province. In addition, XM (38.9%) and SSQ (33.3%) derived air masses from the Shaanxi Province, while some cluster (33.3%) in DF originated from the western provinces (starting from Gansu Province and passing over Shaanxi Province). The lowest $PM_{2.5}$ concentrations were observed in XM and DF (354.4 μg m^{-3} and 362.4 μg m^{-3}, respectively), which suggest that these sites are relatively cleaner than the other examined areas.

PSCF Results

Combined with the backward trajectory analysis, the spatial distribution of potential $PM_{2.5}$ source regions and transportation paths of SSQ are shown in Fig. 9. The potential sources with WPSCF values of higher than 0.4 were mainly distributed northeast (Puyang, Hebi and Xinxiang) and east (Kaifeng) of SSQ. These findings indicate that the migration of atmospheric pollutants in the agricultural areas of Henan Province has a great impact on the $PM_{2.5}$ pollution in urban areas. In addition, the WPSCF value of Nanyang above 0.7, thereby suggesting that the long-distance transmission of pollution sources also contributes to the $PM_{2.5}$ pollution in SSQ.

Health Risk Assessment

The carcinogenic risks of toxic elements in three exposure pathways from different pollution sources in the five sampling sites are shown in Tables S4–S5. The health risks of As (9.7×10^{-5} to 2.6×10^{-4} for children and 4.9×10^{-5} to 1.3×10^{-4} for adults) and Pb (5.7×10^{-6} to 9.8×10^{-6} for children and 2.9×10^{-6} to 5.0×10^{-6} for adults) were mainly accumulated through intake. Ni was mainly distributed through the intake (6.7×10^{-5} to 1.1×10^{-4} for children and 3.4×10^{-5} to 5.6×10^{-5} for adults) and dermal channels (4.7×10^{-5} to 7.7×10^{-5} for children and 3.4×10^{-5} to 5.6×10^{-5} for adults). The carcinogenic risks values of all elements for children were higher than adult via intake and dermal exposure at all sites, while children were below adult via inhalation. The carcinogenic risk values of As from ZM, XM, SSQ, and HKG via ingestion for both children and adults (except for HKG) were higher than 1.0×10^{-4}, thereby indicating a serious potential cancer risk. Meanwhile, the carcinogenic risk values of Pb and Ni from all sampling sites via inhalation were lower than 1.0×10^{-6}, thereby implying that the carcinogenic risk can be ignored.

The non-carcinogenic risks of toxic elements (V, Cu, As, Mn, Zn, Pb, and Ni) in three exposure pathways from different pollution sources in the five sampling sites are shown in Table S6–S7. The highest cumulative HQ values of As (2.7 to 7.2 for children and 3.4×10^{-1} to 9.1×10^{-1} for adults) and Pb (2.4 to 4.1 for children and 3.0×10^{-1} to 5.2×10^{-1} for adults) were mainly distributed in the intake pathway. Meanwhile, the HQ values of V, Cu, Mn, Zn, and Ni via the three exposure pathways were all below the safety level of HQ = 1, thereby suggesting that their potential non-carcinogenic risk could be ignored. The HQ values of As and Pb for children via ingestion were above the safety level of HQ = 1, thereby indicating the serious non-carcinogenic risks of these elements.

The HI_{ing} (ingestion) values of the toxic elements in the five sampling sites ranged from 6.0 (DF) to 12.1 (ZM) for children and from 0.8 (DF) to 1.5 (ZM) for adults. These values exceed the safety level (except for the HI_{ing} value in DF). Meanwhile, the HIder (dermal) values of these elements ranged from 0.8 (DF) to 1.3 (ZM) for children, which were above the safety level (except for the HI_{der} value in DF), thereby suggesting that the potential non-carcinogenic risk of these elements warrants further attention. The HI_{inh} (inhalation) values were below the safety level in all five sampling sites, thereby indicating that the non-carcinogenic risk of these elements can be ignored.

Each element in the five sampling sites contributes a

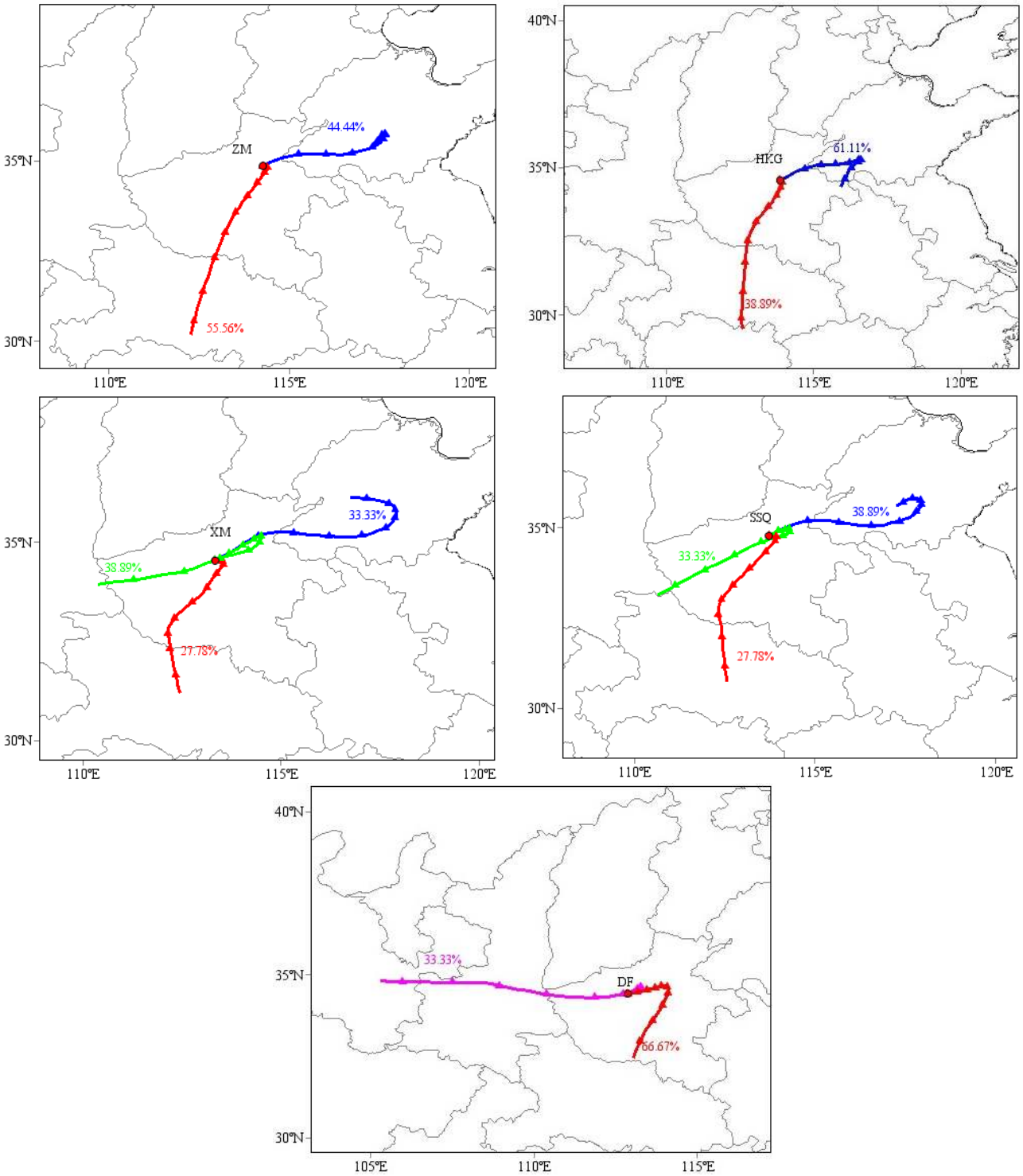

Fig. 8. The results of 48-hour backward air trajectories for December 18–20, 2016 arrived at five sampling sites in Zhengzhou and the altitude was set at 500 m.

different source of health risk via three exposure pathways. The health risk values of V, Cu, and Zn were mainly attributed to traffic exhaust, those of Pb were mainly related to traffic exhaust and coal combustion, those of Ni were mainly attributed to industrial exhaust, those of As were mainly related to coal combustion, and those of Mn were mainly attributed to dust and traffic exhaust. Therefore, the emission of these elements should be reduced to minimize their potential risks to human health.

CONCLUSION

The mass concentrations, chemical compositions, source apportionment, and health risk assessment of $PM_{2.5}$ in the

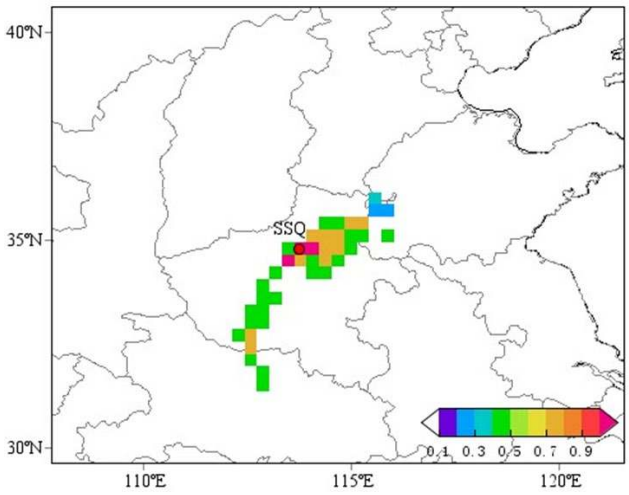

Fig. 9. Spatial distributions of PSCF for $PM_{2.5}$ at SSQ site.

rural, urban, traffic, industrial, and scenic sites of Zhengzhou were examined from February to December of 2016.

The annual mean concentration of $PM_{2.5}$ in these five sites was 119 μg m^{-3}, and the WSIIs, carbonaceous species (EC and OC), and elements accounted for 47.7%, 14.4%, and 9.6% of the $PM_{2.5}$ concentration in Zhengzhou during the sampling period, respectively. The results of CDs indicated that the situation in DF was significantly different from that in the other sites. $PM_{2.5}$, OC, EC, and WSIIs, except for F^-, Ca^{2+}, and Mg^{2+}, showed a relatively homogeneous spatial distribution. The NO_3^-/SO_4^{2-} in the heavy pollution period (December 18–20, 2016) significantly decreased along with increasing $PM_{2.5}$ concentrations, thereby suggesting that stationary sources might have important effects on the $PM_{2.5}$ concentrations during the heavy pollution period. The annual OC/EC ratio was 8.3, which implies the possible presence of SOC.

PMF model was used to identify the six main sources of $PM_{2.5}$ in Zhengzhou, namely, dust (15.1%), coal combustion (17.6%), secondary aerosol (35.1%), vehicle traffic (17.3%), industry (7.3%), and biomass burning (7.7%). The results of the backward trajectory analysis reveal that the long-range transmission of pollutants in Zhengzhou mainly originated from the Shandong, Hubei, and Shaanxi Provinces. The results of the PSCF analysis also identified Puyang, Hebi, Xinxiang, and Kaifeng as potential sources of $PM_{2.5}$ pollutants.

The non-carcinogenic and carcinogenic risk values of all elements from the five sampling sites through ingestion and dermal pathways were higher among children than adults, while through the inhalation pathway were higher among adults than children. As and Ni have the highest carcinogenic risk while As and Pb have the highest non-carcinogenic risk for both children and adults through all three pathways. The As in HKG, ZM, XM, and SSQ can bring carcinogenic risks for children through ingestion, while in ZM, XM, and SSQ can bring carcinogenic risk for adults. Meanwhile, the Pb in all five sampling sites produces an intolerable non-carcinogenic risk for children via ingestion.

ACKNOWLEDGEMENTS

The study was supported by the financial support from the National Natural Science Foundation of China (51808510, 51778587), National Key Research and Development Program of China (2017YFC0212400), Natural Science Foundation of Henan Province of China (162300410255), Foundation for University Young Key Teacher by Henan Province (2017GGJS005), Outstanding Young Talent Research Fund of Zhengzhou University (1421322059) and Science and technology planning project of Transportation in Henan Province (2016Y2-2, 2018J3). Authors would like to appreciate those assisting in analysis: Shiguang Duan, Shenbo Wang, and Zhe Dong.

SUPPLEMENTARY MATERIAL

Supplementary data associated with this article can be found in the online version at http://www.aaqr.org.

REFERENCES

Aldabe, J., Elustondo, D., Santamaría, C., Lasheras, E., Pandolfi, M., Alastuey, A., Querol, X. and Santamaría, J.M. (2011). Chemical characterisation and source apportionment of $PM_{2.5}$ and PM_{10} at rural, urban and traffic sites in Navarra (North of Spain). *Environ. Res.* 102: 191–205.

Argyropoulos, G., Grigoratos, T., Voutsinas, M. and Samara, C. (2013). Concentrations and source apportionment of PM_{10} and associated elemental and ionic species in a lignite-burning power generation area of southern Greece. *Environ. Sci. Pollut. Res.* 20: 7214–7230.

Arimoto, R., Duce, R.A., Savoie, D.L., Prospero, J.M., Talbot, R., Cullen, J.D., Tomza, U., Lewis, N.F. and Ray, B.J. (1996). Relationships among aerosol constituents from Asia and the North Pacific during PEM-West A. *J. Geophys. Res.* 101: 2011–2023.

Betha, R., Behera, S.N. and Balasubramanian, R. (2014). 2013 Southeast Asian smoke haze: Fractionation of particulate-bound elements and associated health risk. *Environ. Sci. Technol.* 48: 4327–4335.

Bhangare, R.C., Ajmal, P.Y., Sahu, S.K., Pandit, G.G. and Puranik, V.D. (2011). Distribution of trace elements in coal and combustion residues from five thermal power plants in India. *Int. J. Coal Geol.* 86: 349–356.

Brown, S.G., Eberly, S., Paatero, P. and Norris, G.A. (2015). Methods for estimating uncertainty in PMF solutions: Examples with ambient air and water quality data and guidance on reporting PMF results. *Sci. Total Environ.* 518–519: 626–635.

Bytnerowicz, A., Omasa, K. and Paoletti, E. (2007). Integrated effects of air pollution and climate change on forests: A northern hemisphere perspective. *Environ. Pollut.* 147: 438–445.

Cesari, D., Benedetto, D.G.E., Bonasoni, P., Busetto, M., Dinoi, A., Merico, E., Chirizzi, D., Cristofanelli, P., Donateo, A., Grasso, F.M., Marinoni, A., Pennetta, A. and Contini, D. (2017). Seasonal variability of $PM_{2.5}$ and PM_{10}

composition and sources in an urban background site in southern Italy. *Sci. Total Environ.* 612: 202–213.

Chan, Y.C., Simpson, R.W., Mctainsh, G.H., Vowles, P.D., Cohen, D.D. and Bailey, G.M. (1997). Characterisation of chemical species in $PM_{2.5}$ and PM_{10} aerosols in Brisbane, Australia. *Atmos. Environ.* 31: 3773–3785.

Charlesworth, S., Miguel, E.D. and Ordóñez, A. (2011). A review of the distribution of particulate trace elements in urban terrestrial environments and its application to considerations of risk. *Environ. Geochem. Health* 33: 103–123.

Chen, Y., Xie, S.D., Luo, B. and Zhai, C.Z. (2017). Particulate pollution in urban Chongqing of southwest China: Historical trends of variation, chemical characteristics and source apportionment. *Sci. Total Environ.* 584–585: 523–534.

Contini, D., Belosi, F., Gambaro, A., Cesari, D., Stortini, A.M. and Bove, M.C. (2012). Comparison of PM_{10} concentrations and metal content in three different sites of the Venice lagoon: An analysis of possible aerosol sources. *J. Environ. Sci.* 24: 1954–1965.

Contini, D., Cesari, D., Conte, M. and Donateo, A. (2016). Application of PMF and CMB receptor models for the evaluation of the contribution of a large coal-fired power plant to PM_{10} concentrations. *Sci. Total Environ.* 560–561: 131–140.

Deng, L.Q., Li, H., Cai, F.H., Lun, X.X., Chen, Y.Z., Wang, F.W. and Ni, R.X. (2011). Pollution characteristics of the atmospheric fine particles and related gaseous pollutants in the northeastern urban area of Beijing. China. *Environ. Sci.* 31: 1064–1070.

Deng, X.L., Shi, C.E., Wu, B.W., Yang, Y.J., Jin, Q., Wang, H.L., Zhu, S. and Yu, C.X. (2016). Characteristics of the water-soluble components of aerosol particles in Hefei, China. *J. Environ. Sci.* 42: 32–40.

Diapouli, E., Manousakas, M., Vratolis, S., Vasilatou, V., Maggos, Th., Saraga, D., Grigoratos, Th., Argyropoulos, G., Voutsa, D., Samara, C. and Eleftheriadis, K. (2017). Evolution of air pollution source contributions over one decade, derived by PM_{10}, and $PM_{2.5}$, source apportionment in two metropolitan urban areas in Greece. *Atmos. Environ.* 164: 416–430.

Du, W.J., Zhang, Y.R., Chen, Y.T., Xu, L.L., Chen, J.S., Deng, J.J., Hong, Y.W. and Xiao, H. (2017). Chemical characterization and source apportionment of $PM_{2.5}$ during spring and winter in the Yangtze River Delta, China. *Aerosol Air Qual. Res.* 17: 2165–2180.

Feng, J.L., Hu, J.C., Xu, B.H., Hu, X.L., Sun, P., Han, W.L., Gu, Z.P., Yu, X.M. and Wu, M.H. (2015). Characteristics and seasonal variation of organic matter in $PM_{2.5}$, at a regional background site of the Yangtze River Delta region, China. *Atmos. Environ.* 123: 288–297.

Gao, Y., Guo, X.Y., Ji, H.B., Li, C., Ding, H.J., Briki, M., Tang, L. and Zhang, Y. (2016). Potential threat of heavy metals and PAHs in $PM_{2.5}$ in different urban functional areas of Beijing. *Atmos. Res.* 178–179: 6–16.

Garg, B.D., Cadle, S.H., Mulawa, P.A., Groblicki, P.J., Laroo, C. and Parr, G.A. (2000). Brake wear particulate matter emissions. *Environ. Sci. Technol.* 34: 4463–4469.

Geng, N.B., Wang, J., Xu, Y.F., Zhang, W.D., Chen, C. and Zhang, R.Q. (2013). $PM_{2.5}$ in an industrial district of Zhengzhou, China: Chemical composition and source apportionment. *Particuology* 11: 99–109.

Gu, J.X., Bai, Z.P., Li, A.X., Wu, L.P., Xie, Y.Y., Lei, W.F., Dong, H.Y. and Zhang, X. (2011). Chemical composition of $PM_{2.5}$ during winter in Tianjin, China. *Particuology* 9: 215–221.

Han, Y.J., Kim, H.W., Cho, S.H., Kim, P.R. and Kim, W.J. (2015). Metallic elements in $PM_{2.5}$ in different functional areas of Korea: Concentrations and source identification. *Atmos. Res.* 153: 416–428.

Hsu, C.Y., Chiang, H.C., Lin, S.L., Chen, M.J., Lin, T.Y. and Chen, Y.C. (2016). Elemental characterization and source apportionment of PM_{10} and $PM_{2.5}$ in the western coastal area of central Taiwan. *Sci. Total Environ.* 541: 1139–1150.

Hsu, C.Y., Chiang, H.C., Chen, M.J., Chuang, C.Y., Tsen, C.M., Fang, G.C., Tsai, Y.I., Chen, N.T., Lin, T.Y., Lin, S.L. and Chen, Y.C. (2017). Ambient $PM_{2.5}$ in the residential area near industrial complexes: Spatiotemporal variation, source apportionment, and health impact. *Sci. Total Environ.* 590–591: 204–214.

Hsu, S.C., Liu, S.C., Tsai, F., Engling, G., Lin, I.I., Chou, C.K. C., Kao, S.J., Lung, S.C.C., Chan, C.Y., Lin, S.C., Huang, J.C., Chi, K.H., Chen, W.N., Lin, F.J., Huang, C.H., Kuo, C.L., Wu, T.C. and Huang, Y.T. (2010). High wintertime particulate matter pollution over an offshore island (Kinmen) off southeastern China: An overview. *J. Geophys. Res.* 115: D17309.

Huang, T., Chen, J., Zhao, W.T., Cheng, J.X. and Cheng, S.G. (2016). Seasonal variations and correlation analysis of water-soluble inorganic ions in $PM_{2.5}$ in Wuhan, 2013. *Atmosphere* 7: 49.

Huang, X.J., Liu, Z.R., Liu, J.Y., Hu, B., Wen, T.X., Tang, G.Q., Zhang, J.K., Wu, F.K., Ji, D.S., Wang, L.L. and Wang, Y.S. (2017). Chemical characterization and source identification of $PM_{2.5}$ at multiple sites in the Beijing-Tianjin-Hebei region, China. *Atmos. Chem. Phys.* 17: 12941–12962.

Jiang, N., Guo, Y., Wang, Q., Kang, P.R., Zhang, R.Q. and Tang, X.Y. (2017). Chemical composition characteristics of $PM_{2.5}$ in three cities in Henan, central China. *Aerosol Air Qual. Res.* 17: 2367–2380.

Jiang, N., Dong, Z., Xu, Y. Q., Yu, F., Yin, S. S., Zhang, R. Q. and Tang, X.Y. (2018a). Characterization of PM_{10} and $PM_{2.5}$ source profiles for fugitive dust in Zhengzhou, China. *Aerosol Air Qual. Res.* 18: 314–329.

Jiang, N., Duan, S.G., Yu, X., Zhang R.Q. and Wang, K. (2018b). Comparative major components and health risks of toxic elements and polycyclic aromatic hydrocarbons of $PM_{2.5}$ in winter and summer in Zhengzhou: Based on three-year data. *Atmos. Res.* 213: 173–184.

Jiang, N., Li, Q., Su, F.C., Wang, Q., Yu, X., Kang, P.R., Zhang, R.Q. and Tang, X.Y. (2018c). Chemical characteristics and source apportionment of $PM_{2.5}$, between heavily polluted days and other days in Zhengzhou, China. *J. Environ. Sci.* 66: 188–198.

Jiang, N., Wang, K., Yu, X., Su, F.C., Yin S.S., Li, Q. and

Zhang R.Q. (2018d). Chemical characteristics and source apportionment by two receptor models of size-segregated aerosols in an emerging megacity in China. *Aerosol Air Qual. Res.* 18: 1375–1390.

Jiang, N., Yin, S.S., Guo, Y., Li, J.Y., Kang, P.R., Zhang, R.Q. and Tang, X.Y. (2018e). Characteristics of mass concentration, chemical composition, source apportionment of $PM_{2.5}$ and PM_{10} and health risk assessment in the emerging megacity in China. *Atmos. Pollut. Res.* 9: 309–321.

Jiang, N., Li, L.P., Wang, S.S., Li, Q., Dong, Z., Duan, S.G., Zhang, R.Q. and Li, S.L. (2019a). Variation tendency of pollution characterization, sources, and health risks of $PM_{2.5}$-bound polycyclic aromatic hydrocarbons in an emerging megacity in China: Based on three-year data. *Atmos. Res.* 217: 81–92.

Jiang, N., Liu, X.H., Wang, S.S., Yu, X., Yin S.S., Duan, S.G., Wang, S.B., Zhang, R.Q. and Li, S.L. (2019b). Pollution characterization, source identification, and health risks of atmospheric-particle-bound heavy metals in PM_{10} and $PM_{2.5}$ at multiple sites in an emerging megacity in the central region of China. *Aerosol Air Qual. Res.* 19: 247–271.

Kuo, C.Y., Yang, H.J., Chiang, Y.C., Lai, D.J., Shen, Y.H. and Liu, P.M. (2014). Concentration and composition variations of metals in the outdoor PM_{10} of elementary schools during river dust episodes. *Environ. Sci. Pollut. Res. Int.* 21: 12354–12363.

Lan, Y., Yang, L.X., Qi, Y., Chao, Y., Dong, C., Meng, C.P., Sui, X., Yang, F., Lu, Y.L. and Wang, W.X. (2016). Sources apportionment of $PM_{2.5}$ in a background site in the North China Plain. *Sci. Total Environ.* 541: 590–598.

Li, H.M., Wang, Q.G., Yang, M., Li, F.Y., Wang, J.H., Sun, Y.X., Wang, C., Wu, H.F. and Qian, X. (2016). Chemical characterization and source apportionment of $PM_{2.5}$, aerosols in a megacity of Southeast China. *Atmos. Res.* 181: 288–299.

Li, Q., Jiang, N., Yu, X., Dong, Z., Duan, S.G. and Zhang, R.Q. (2019). Spatial-seasonal distribution and source apportionment of $PM_{2.5}$-bound polycyclic aromatic hydrocarbons in Zhengzhou in 2016. *Atmos. Res.* 216: 65–75.

Liu, B.S., Wu, J.H., Zhang, J.Y., Wang, L., Yang, J.M., Liang, D.N., Dai, Q.L., Bi, X.H., Feng, Y.C., Zhang, Y.F. and Zhang, Q.X. (2017). Characterization and source apportionment of $PM_{2.5}$ based on error estimation from EPA PMF5.0 model at a medium city in China. *Environ. Pollut.* 222: 10–22.

Liu, B., Cheng, Y., Zhou, M., Liang, D., Dai, Q., Wang, L., Jin, W., Zhang, L., Ren, Y., Zhou, J., Dai, C., Xu, J., Wang, J., Feng, Y. and Zhang, Y. (2018). Effectiveness evaluation of temporary emission control action in 2016 in winter in Shijiazhuang, China. *Atmos. Chem. Phys.* 18: 7019–7039.

Lough, G.C., Schauer, J.J., Park, J.S., Shafer, M.M., Deminter, J.T. and Weinstein, J.P. (2005). Emissions of metals associated with motor vehicle roadways. *Environ. Sci. Technol.* 39: 826–836.

Meng, C.C., Wang, L.T., Zhang, F.F., Wei, Z., Ma, S.M., Ma, X. and Yang, J. (2016). Characteristics of concentrations and water-soluble inorganic ions in $PM_{2.5}$, in Handan city, Hebei province, China. *Atmos. Res.* 171: 133–146.

Ministry of Environmental Protection of the People's Republic of China (2017). Report on the state of the environment in China in 2016. http://english.mep.gov.cn/Resources/Reports/soe/ReportSOE/201709/P020170929573904364594.pdf.

Mohsenibandpi, A., Eslami, A., Shahsavani, A., Khodagholi, F. and Alinejad, A. (2017). Physicochemical characterization of ambient $PM_{2.5}$ in Tehran air and its potential cytotoxicity in human lung epithelial cells (A549). *Sci. Total Environ.* 593–594: 182–190.

Paatero, P. and Tapper, U. (1994). Positive matrix factorization: A non-negative factor model with optimal utilization of error estimates of data values. *Environmetrics* 5: 111–126.

Paatero, P. (1997). Least squares formulation of robust non-negative factor analysis. *Chemom. Intell. Lab. Syst.* 37: 23–35.

Park, S.S. and Kim, Y.J. (2004). $PM_{2.5}$ particles and size-segregated ionic species measured during fall season in three urban sites in Korea. *Atmos. Environ.* 38: 1459–1471.

Perrone, M.G., Gualtieri, M., Ferrero, L., Porto, C.L., Udisti, R., Bolzacchini, E. and Camatini, M. (2010). Seasonal variations in chemical composition and in vitro biological effects of fine PM from Milan. *Chemosphere* 78: 1368–1377.

Pope, III, C.A. and Dockery, D.W. (2006). Health effects of fine particulate air pollution: Lines that connect. *J. Air Waste Manage. Assoc.* 56: 709–742.

Squizzato, S., Masiol, M., Brunelli, A., Pistollato, S., Tarabotti, E., Rampazzo, G. and Pavoni1, B. (2013). Factors determining the formation of secondary inorganic aerosol: A case study in the Po Valley (Italy). *Atmos. Chem. Phys.* 13: 1927–1939.

Tan, J.H., Duan, J.C., Ma, Y.L., He, K.B., Cheng, Y., Deng, S.X., Huang, Y.L. and Situ, S.P. (2016). Long-term trends of chemical characteristics and sources of fine particle in Foshan city, Pearl River Delta: 2008-2014. *Sci. Total Environ.* 565: 519–528.

Tao, J., Gao, J., Zhang, L., Zhang, R., Che, H., Zhang, Z., Lin, Z., Jing, J., Gao, J. and Hsu, S.C. (2014). $PM_{2.5}$ pollution in a megacity of southwest China: Source apportionment and implication. *Atmos. Chem. Phys.* 14: 8679–8699.

Taylor, S.R. (1964). Trace element abundances and the chondritic Earth model. *Geochim. Cosmochim. Ac*. 28: 1989–1998.

Turpin, B.J. and Huntzicker, J.J. (1995). Identification of secondary organic aerosol episodes and quantitation of primary and secondary organic aerosol concentrations during SCAQS. *Atmos. Environ.* 29: 3527–3544.

Turpin, B.J. an, Lim, H.J. (2001). Species contributions to $PM_{2.5}$ mass concentrations: Revisiting common assumptions for estimating organic mass. *Aerosol Sci. Technol.* 35: 602–610.

U.S. EPA (2014). Positive Matrix Factorization (PMF) 5.0

Fundamentals and User Guide.Office of Research and Development, Washington, DC. https://www.epa. gov/sites/production/files/2015-02/documents/pmf_5.0_user_guide.pdf.

Viana, M., Querol, X., Alastuey, A., Gil, J.I. and Menéndez, M. (2006). Identification of PM sources by principal component analysis (PCA) coupled with wind direction data. *Chemosphere* 65: 2411–2418.

Wang, S., Yan, Q., Yu, F., Wang, Q., Yang, L., Zhang, R. and Yin, S. (2018). Distribution and source of chemical elements in size-resolved particles in Zhengzhou, China: effects of regional transport. *Aerosol Air Qual. Res.* 18: 371–385.

Wang, W., Primbs, T., Tao, S. and Simonich, S.L.M. (2009). Atmospheric particulate matter pollution during the 2008 Beijing Olympics. *Environ. Sci. Technol.* 43: 5314–5320.

Wang, X., Bi, X., Sheng, G. and Fu, J. (2006a). Chemical composition and sources of PM_{10} and $PM_{2.5}$ aerosols in Guangzhou, China. *Environ. Monit. Assess.* 119: 425–439.

Wang, Y., Zhuang, G.S., Zhang, X.Y., Huang, K., Xu, C., Tang, A.H., Chen, J.M. and An, Z.S. (2006b). The ion chemistry, seasonal cycle, and sources of $PM_{2.5}$ and TSP aerosol in Shanghai. *Atmos. Environ.* 40: 2935–2952.

Wang, Y.N., Jia, C.H., Tao, J., Zhang, L.M., Liang, X.X., Ma, J.M., Gao, H., Huang, T. and Zhang, K. (2016). Chemical characterization and source apportionment of $PM_{2.5}$ in a semi-arid and petrochemical-industrialized city, Northwest China. *Sci. Total Environ.* 573: 1031–1040.

Xiao, H.Y. and Liu, C.Q. (2004). Chemical characteristics of water-soluble components in TSP over Guiyang, SW China, 2003. *Atmos. Environ.* 38: 6297–6306.

Xu, L., Yu, Y., Yu, J., Chen, J., Niu, Z., Yin, L.Q., Zhang, F.W., Liao, X. and Chen, Y.T. (2013). Spatial distribution and sources identification of elements in $PM_{2.5}$ among the coastal city group in the Western Taiwan Strait region, China. *Sci. Total Environ.* 442: 77–85.

Yang, F., Tan, J., Zhao, Q., Du, Z., He, K., Ma, Y., Duan, F., Chen, G. and Zhao, Q. (2011). Characteristics of $PM_{2.5}$ speciation in representative megacities and across China. *Atmos. Chem. Phys.* 11: 5207–5219.

Yang, Y.R., Liu, X.G., Qu, Y., An, J.L., Jiang, R., Zhang, Y.H., Sun, Y.L., Wu, Z.J., Zhang, F., Xu, W.Q. and Ma, Q.X. (2015). Characteristics and formation mechanism of continuous hazes in china: A case study during the autumn of 2014 in the north China plain. *Atmos. Chem. Phys.* 15: 8165–8178.

Yao, X.H., Chan, C.K., Fang, M., Cadle, S., Chan, T., Mulawa, P., He, K.B. and Ye, B.M. (2002). The water-soluble ionic composition of $PM_{2.5}$ in Shanghai and Beijing, China. *Atmos. Environ.* 36: 4223–4234.

Yin, L.Q., Niu, Z.C., Chen, X.Q., Chen, J.S., Zhang, F.W. and Xu, L.L. (2014). Characteristics of water-soluble inorganic ions in $PM_{2.5}$ and $PM_{2.5\text{-}10}$ in the coastal urban agglomeration along the western Taiwan Strait Region, China. *Environ. Sci. Pollut. Res. Int.* 21: 5141–5156.

Yu, F., Wang, Q., Yan, Q., Jiang, N., Wei, J., Wei, Z. and Yin, S. (2018). Particle size distribution, chemical composition and meteorological factor analysis: A case study during wintertime snow cover in Zhengzhou, China. *Atmos. Res.* 202: 140–147.

Yuan, Z.B., Yu, J.Z., Lau, A.K.H., Louie, P.K.K. and Fung, J.C.H. (2005). Application of positive matrix factorization in estimating aerosol secondary organic carbon in Hong Kong and insights into the formation mechanisms. *Atmos. Chem. Phys.* 5: 5299–5324.

Zhang, F., Cheng, H.R., Wang, Z.W., Lv, X.P., Zhu, Z.M., Zhang, G. and Wang, X.M. (2016). Fine particles ($PM_{2.5}$) at a CAWNET background site in Central China: Chemical compositions, seasonal variations and regional pollution events. *Atmos. Environ.* 86: 193–202.

Zhang, F., Wang, Z.W., Cheng, H.R., Lv, X.P., Gong, W., Wang, X.M. and Zhang, G. (2015). Seasonal variations and chemical characteristics of $PM_{2.5}$ in Wuhan, central China. *Sci. Total Environ.* 518–519: 97–105.

Zhang, R.J., Cao, J.J., Lee, S.C., Shen, Z.X. and Ho, K.F. (2007). Carbonaceous aerosols in PM_{10} and pollution gases in winter in Beijing. *J. Environ. Sci.* 19: 564–571.

Zhang, R., Jing, J., Tao, J., Hsu, S.C., Wang, G., Cao, J., Lee, C.S.L., Zhu, L., Chen, Z. and Zhao, Y. (2013). Chemical characterization and source apportionment of $PM_{2.5}$ in Beijing: Seasonal perspective. *Atmos. Chem. Phys.* 13: 7053–7074.

Zhang, X.Y., Wang, Y.Q., Zhang, X.C., Guo, W. and Gong, S.L. (2008). Carbonaceous aerosol composition over various regions of China during 2006. *J. Geophys. Res.* 113: D14111.

Zheng, J., Tan, M.G., Shibata, Y., Tanaka, A., Li, Y., Zhang, G.L., Zhang, Y.M. and Shan, Z. (2004). Characteristics of lead isotope ratios and elemental concentrations in PM_{10} fraction of airborne participate matter in Shanghai after the phase-out of leaded gasoline. *Atmos. Environ.* 38: 1191–1200.

Zhou, X.H., Cao, Z.Y., Ma, Y.J., Wang, L.P., Wu, R.D. and Wang, W.X. (2016). Concentrations, correlations and chemical species of $PM_{2.5}/PM_{10}$ based on published data in China: Potential implications for the revised particulate standard. *Chemosphere* 144: 518–526.

ZMBS (2017). Zhengzhou Municipal Bureau of Statistics. http://tjj.zhengzhou.gov.cn/, Last Access: Dec. 2017.

ZMEPB (2016). Zhengzhou Municipal Environmental Protection Bureau. The closed and production suspended progress of environmental illegal construction projects in Zhengzhou http://www.zzepb.gov.cn/Article/Content/?id=35269. (in Chinese).

Received for review, February 15, 2019
Revised, May 20, 2019
Accepted, September 2, 2019